^{35}Cl NQR Relaxation and Hydrogen Bond in Some Chloral Hemiacetals *

Masao Hashimoto and Shuji Matsumoto
Department of Chemistry, Faculty of Science, Kobe University, Nadaku, Kobe 657, Japan

Masakazu Kunitomo
Department of Physics, Faculty of Science, Kobe University, Nadaku, Kobe 657, Japan

Haruo Niki
Department of Physics, Division of General Education, University of the Ryukyus, Nishihara, Okinawa 903-01, Japan

Hirotaka Odahara and Katsuji Tamaki
Department of Physics, College of Science, University of the Ryukyus, Nishihara, Okinawa 903-01, Japan

Z. Naturforsch. **49a**, 279–285 (1994); received August 16, 1993

The crystal structure of chloral ethylhemiacetal has been determined at 291 K: monoclinic, space group C_2^2–$P2_1$, $Z = 2$, $a = 854.5(1)$, $b = 594.0(3)$, $c = 853.3(1)$ pm, $\beta = 108.30(2)°$, $R = 0.0962$. A sharp decrease of the spin lattice relaxation time T_1 found for the ^{35}Cl NQR of the CCl_3 groups in chloral methyl-, ethyl- and n-heptylhemiacetals is attributed to the onset of reorientation of the group over a potential barrier of ca. 39, 37, and 32 kJ/mol, respectively. An unusual T_1 vs. $1/T$ curve with a T_1 minimum superimposed on the sharp decrease of T_1 due to the reorientation was observed for each of the three ^{35}Cl NQR lines of nHp-CH. This phenomenon is tentatively ascribed to a fluctuation of EFG caused by jumping motion of the hydrogen atoms in the OH groups.

Key words: Crystal structure, Hydrogen bond, Chlorine NQR, Spin lattice relaxation.

Introduction

In trichloromethyl derivatives, the spin lattice relaxation time (T_1) of the chlorine NQR corresponding to the CCl_3 group drops often sharply with increasing temperature in a certain temperature range far below the melting point. The phenomenon has been attributed to fluctuations of the electric field gradient (EFG) caused by the reorientation of the CCl_3 group [1].

In the course of ^{35}Cl NQR studies on chloral hemiacetals ($Cl_3CCH(OH)O.R$) we found that chloral n-butylhemiacetal (nB-CH) and chloral cyclohexylhemiacetal (cycHx-CH) exhibit an unusual T_1 vs. $1/T$ relation with a T_1 minimum superimposed on the sharp decrease in T_1 [2, 3]. A chain structure of molecules formed by intermolecular O–H···O hydrogen bonds (H-bond) is common to these crystals, and a dynamic disorder of hydrogen atoms in the OH groups has been proposed as a possible cause of the T_1 minimum. In solid chloral 4-chlorobenzylhemiacetal (pCB-CH), however, the unusual behavior of T_1 seemed to be absent at temperatures between 77 and 300 K in spite of its similar H-bonded chain structure [4].

In this work, we studied the temperature dependence of T_1 of the ^{35}Cl NQR in chloral methyl-, ethyl-, and n-heptylhemiacetal to obtain further information on the correlation between the unusual T_1 behavior and the molecular motions in the crystals of chloral hemiacetals. Single crystal X-ray work was also carried out for the ethyl derivative at room temperature.

Experimental

Preparation

Chloral methylhemiacetal (Me-CH), chloral ethylhemiacetal (Et-CH) and chloral n-heptylhemiacetal (nHp-CH) were prepared from chloral and the corre-

* Presented at the XIIth International Symposium on Nuclear Quadrupole Resonance, Zürich, July 19–23, 1993.

Reprint requests to Dr. Masao Hashimoto, Department of Chemistry, Faculty of Science, Kobe University, Nadaku, Kobe 657, Japan.

0932-0784 / 94 / 0100-0279 $ 01.30/0. – Please order a reprint rather than making your own copy.

Table 1. Experimental conditions for the crystal structure determination and crystallographic data of Et-CH.

Formula	$C_4H_7Cl_3O_2$
Molecular mass, g/mol	193.4
Crystal habitus	needle
Size/mm^3	0.1 × 0.3 × 0.4
Diffractometer	Rigaku AFC-5
Wavelength, λ/pm	71.073 (Mo-Kα)
$(\sin\theta/\lambda)_{max}$/pm^{-1}	0.0054
Monochromator	graphite (002)
Temperature, T/K	297
Linear absorption coefficient, μ/m^{-1}	1053
Crystal system	monoclinic
Lattice constants a/pm	854.5(1)
b/pm	594.0(3)
c/pm	853.3(1)
β/°	108.30(2)
Volume of the unit cell $V \cdot 10^{-6}$/pm^3	411.2(2)
Space group	C_2^2–$P2_1$
Formula units/unit cell	$Z = 2$
ϱ_{calc}/(Mg m^{-3})	1.563
ϱ_{obs}/(Mg m^{-3})	1.555
Scan	$2\theta/\omega$
Number of measured reflections	652
Symmetry independent reflections	606
Reflections considered ($F_0 > \sigma(F_0)$)	494
Number of free parameters	83
$F(000)$	196
$R(F)$	0.0962
$R_w(F)$	0.0844
S	2.545
Weighting scheme	
$w = (\sigma^2(F_0) + a\lvert F_0\rvert + b\lvert F_0\rvert^2)^{-1}$ for $F_0 > 0$	$a = -0.06213$
$w = 0$ for $F_0 = 0$	$b = 0.00857$
$(\Delta/\sigma)_{max}$	0.3034
Final residual electron densities (e/(0.01 nm)^3) (max./min.)	0.58/−0.58

sponding alcohols by the method described in [5, 6]. Me- and Et-CH were purified by recrystallization from petroleum ether, and nHp-CH from n-hexane.

^{35}Cl NQR

T_1 of the ^{35}Cl NQR in Me- and Et-CH was measured by a commercial pulsed spectrometer (Matec Model 6600). Conventional $180°-\tau-90°$ pulse sequence was used for the determination of T_1. T_1 of the ^{35}Cl NQR in nHp-CH was measured by the pulsed spectrometer reported in [2]. In the lower temperature range, where T_1 is longer than T_2, T_1 was determined by the $90°-\tau-90°-\tau'-180°$ pulse sequence while at higher temperatures the $90°-\tau-90°$ pulse method was applied.

Crystal Structure Analysis

The structure of Et-CH was determined by single crystal X-ray analysis at room temperature using Mo-Kα radiation. The experimental details are given in Table 1. The structure was obtained by the direct method (MULTAN 78) [7] and refined by the least-squares method (HBLS-V) [8]. Anisotropic temperature factors were applied to the nonhydrogen atoms. The positions of hydrogen atoms, except for the one in the OH group, were estimated by calculations and provided with isotropic temperature factors. The position of the hydrogen atom in the OH group was not determined because this was too difficult with a differ-

Table 2. Positional and thermal parameters (with standard deviations) of chloral ethylhemiacetal (Et-CH). The temperature factor exponent has the form: $-(B_{11}h^2 + B_{22}k^2 + B_{33}l^2 + B_{12}hk + B_{13}hl + B_{23}kl)$ for non-hydrogen atoms, $-B_{iso}(\sin^2\theta/\lambda^2)$ for hydrogen atoms. The B_{nm} are given in units of 10^{-10} m^2.

Atom	x/a	y/b	z/c	B_{11} or B_{iso}	B_{22}	B_{33}	B_{12}	B_{13}	B_{23}
Cl(1)	0.8603(6)	0.8994(11)	0.8970(7)	0.0144(7)	0.0362(19)	0.0309(11)	−0.0111(23)	0.0138(15)	−0.0112(27)
Cl(2)	0.7284(5)	0.4517(11)	0.8103(7)	0.0144(7)	0.0277(14)	0.0282(10)	0.0096(10)	0.0152(14)	0.0011(24)
Cl(3)	0.6283(7)	0.8129(13)	0.5780(6)	0.0217(9)	0.0557(26)	0.0217(10)	0.0058(28)	0.0159(16)	0.0161(30)
O1	0.4049(14)	0.6637(26)	0.7685(17)	0.0116(19)	0.0368(49)	0.0310(31)	0.0135(54)	0.0142(43)	0.0042(68)
O2	0.5849(15)	0.7690(28)	1.0207(17)	0.0204(24)	0.0443(62)	0.0297(30)	−0.0142(75)	0.0255(47)	−0.0118(82)
C1	0.6823(20)	0.7451(35)	0.7854(22)	0.0121(27)	0.0323(71)	0.0243(39)	−0.0170(85)	0.0211(56)	−0.0119(93)
C2	0.5393(20)	0.8088(32)	0.8489(21)	0.0135(27)	0.0235(58)	0.0172(31)	−0.0193(73)	0.0064(50−	−0.0147(84)
C3	0.2446(24)	0.7982(65)	0.7254(33)	0.0120(31)	0.0829(154)	0.0434(65)	−0.0018(123)	0.0072(76)	−0.0570(185)
C4	0.1221(25)	0.6163(57)	0.6435(30)	0.0169(38)	0.0763(140)	0.0292(51)	−0.0104(126)	0.0043(74)	−0.0396(158)
H2	0.4838	0.9833	0.8405	5.0					
H3	0.2435	0.9372	0.6399	5.0					
H4	0.2213	0.8651	0.8362	5.0					
H5	−0.0031	0.6875	0.6041	5.0					
H6	0.1290	0.4786	0.7317	5.0					
H7	0.1512	0.5507	0.5354	5.0					

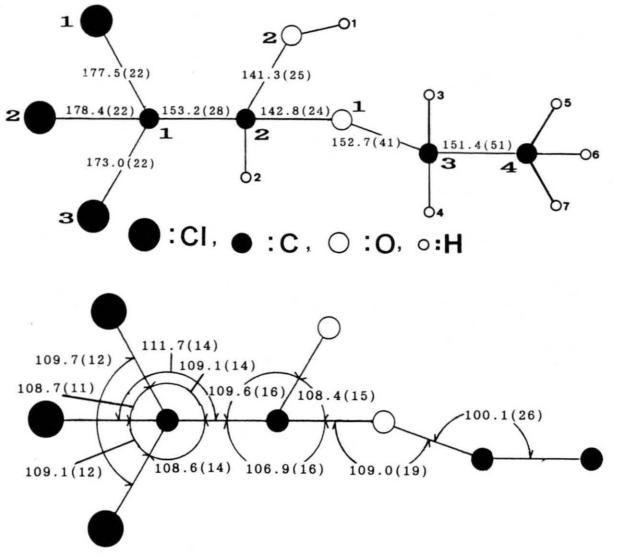

Fig. 1. Bond lengths (top) and bond angles (bottom) of Et-CH.

ence Fourier map. The atomic scattering factors are taken from [9]. All calculations were performed on an ACOS 2020 Computer at the Information Processing Center of Kobe University with the UNICS systems [10].

Crystals of Me-CH are hygroscopic and the X-ray experiment on this compound could not be carried out. The crystal of nHp-CH was found to be damaged by X-ray radiation, and therefore we could not collect the diffraction data required for crystal structure analysis. But the following crystal data of nHp-CH were obtained: monoclinic, space group $C_2^2-P2_1$, $a=1317.4(3)$, $b=584.0(4)$, $c=846.3(1)$ pm, $\beta=94.43(1)°$.

Infrared (IR) Spectrum; Molecular Orbit (MO) Calculations

The IR spectra were recorded on a Hitachi EPI-G2 spectrometer. Since nHp-CH melts just above room temperature, the IR spectrum of this compound was measured with the aid of a conventional cryostat described in [11]. For the MO calculations we used the MNDO method (MOPAC Ver. 6, PM3) [12].

Results

Crystal Structure of Et-CH

Table 1 lists the crystallographic data of Et-CH. The positional and thermal parameters of the atoms

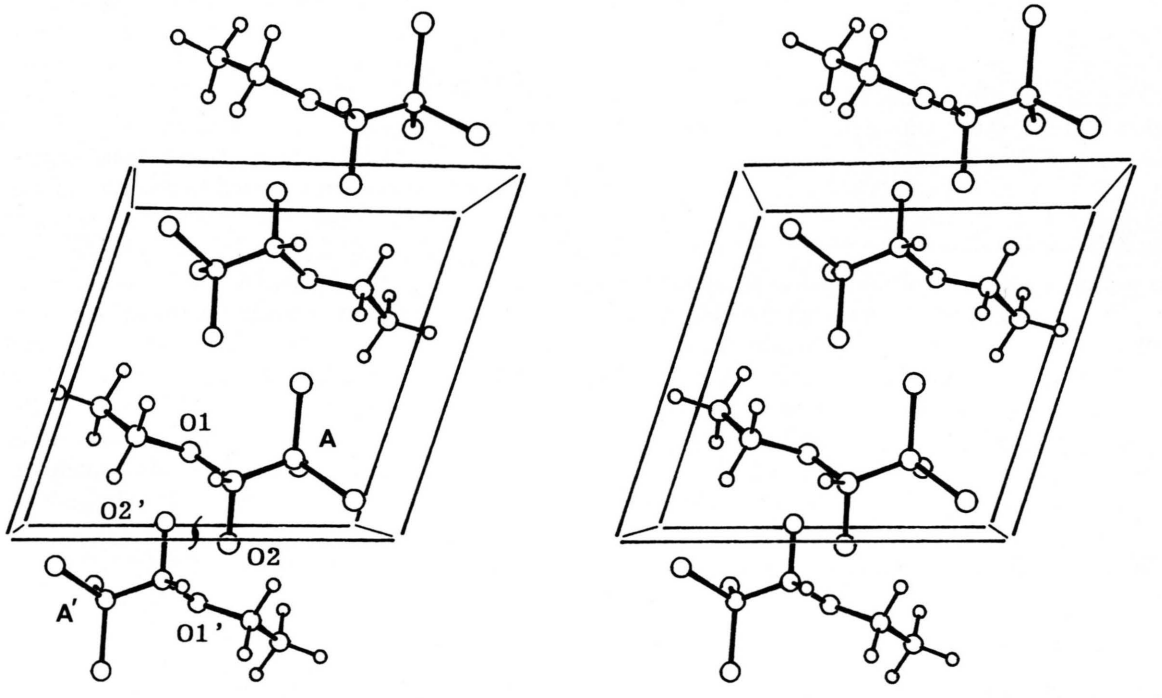

Fig. 2. Crystal structure of Et-CH viewed along the *b* axis (stereo view).

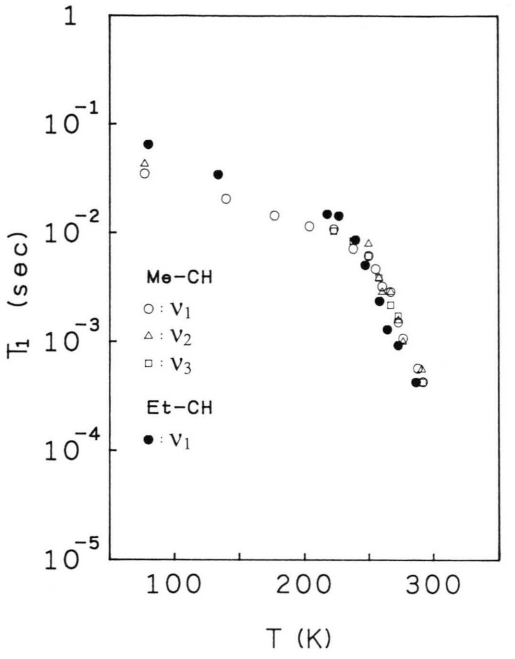

Fig. 3. Temperature dependence of T_1 of ^{35}Cl NQR in Me- and Et-CH.

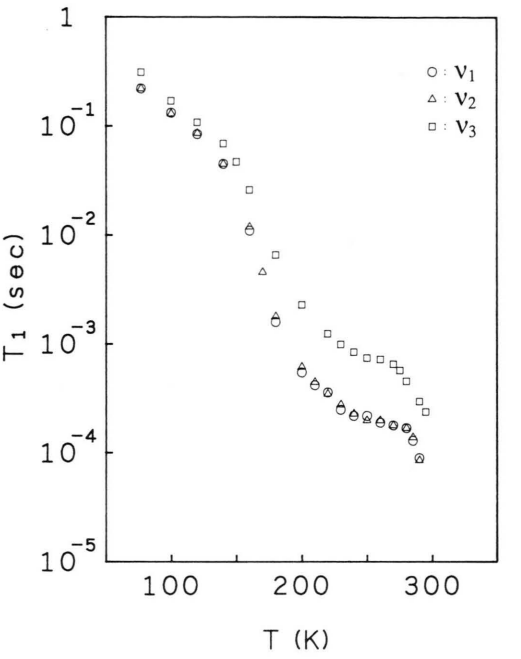

Fig. 4. Temperature dependence of T_1 of ^{35}Cl NQR in nHp-CH.

in the asymmetric unit of the crystal are given in Table 2. The equivalent temperature factors (B_{eq}) were as follows: Cl(1) = 5.7(1), Cl(2) = 5.0(2), Cl(3) = 6.4(2), C(1) = 4.4(6), C(2) = 3.9(5), C(3) = 9.1(10), C(4) = 7.9(9), O(1) = 5.4(5), O(2) = 6.2(4) in units of 10^{-10} m^2.

The bond lengths and bond angles are given in Figure 1. The crystal structure viewed along the *b*-axis is shown in Figure 2.

^{35}*Cl NQR*

It is known that each of the three compounds has three ^{35}Cl NQR lines (ν_{1-3}) and that the NQR signals of Me-CH (m.p. = 318 K), Et-CH (m.p. = 326 K) and nHp-CH (m.p. = 305 K) fade out at ca. 314, 310, and 301 K, respectively [6]. For Me- and Et-CH, T_1 vs. $1/T$ curves are shown in Figure 3. The two NQR lines (ν_3 and ν_2) of Et-CH are close to each other at higher temperatures and hence T_1 was not measured for these lines. The temperature dependences of T_1 of the ^{35}Cl NQR in nHp-CH are shown in Figure 4.

Infrared (IR) Spectrum

The IR band of Et-CH, assigned to the OH stretching vibration (ν_{OH}), is broad and seemed to have two components (ca. 3420 and 3330 cm^{-1}) at room temperature. The ν_{OH} band of nHp-CH has also two components (ca. 3390 and 3300 cm^{-1}).

MO Calculations

In order to estimate the magnitude of the intermolecular H···O interaction in the H-bond system, the MNDO method was applied to a cluster of two Et-CH molecules. The arrangement of the two molecules in the cluster was assumed to be the same as that found in the crystal (A and A′ in Figure 2). The two center energy between the intermolecular H and O atoms (E_{HO}), which corresponds to the strength of the H···O interaction, was calculated as a function of the dihedral angle of C1–C2···O2–H (θ). E_{OH}(H···O1′) showed a minimum at $\theta = 120°$. At the same angle, the E_{OH}(H···O2′) was also minimum. The ratio E_{OH}(H···O2′)/E_{OH}(H···O1′) was ca. 0.44.

Discussion

Crystal Structure

Crystal structures of seven chloral hemiacetals are known [2–4, 13]. The mean values of some selected

bond lengths and bond angles obtained therefrom are as follows: C2–O2 = 139.5, C2–O1 = 139.2, O1–C3 = 145.3 pm, and the angle C2–O1–C3 = 114.7°. Figure 1 shows that the O1–C3 bond length and the bond angle C2–O1–C3 of Et-CH differ significantly from the corresponding mean values. Moreover, the angle O1–C3–C4 of Et-CH is considerably smaller than the tetrahedral angle. These observations are considered to indicate a slight disorder of C3 and C4 in the crystal of Et-CH. The relatively large values of B_{eq} of C3 and C4 seem to support this view.

The crystal structure of Et-CH is characterized by chains of molecules formed by H-bonds running along 2_1 axes (Figure 2). The intermolecular arrangement of –CH(OH)–O– groups in the H-bonded chain of Et-CH is quite similar to those in the six of the seven chloral hemiacetals mentioned above (in the isobutyl derivative, there is a H-bonded dimer of molecules). Since the intermolecular O2···O1′ and O2···O2′ distances of Et-CH are 293.9(23) and 327.6(24) pm, respectively, a bifurcated H-bond is possible as in the cases of some chloral hemiacetals [2–4, 13]. In fact, the results of the present MNDO calculations indicate that there is a significant intermolecular interaction between H and O2′ atoms. This appears to support the presence of the bifurcated H-bond.

A relationship between the O···O distance and the wavenumber of ν_{OH} has been proposed [14]. The wavenumber of ν_{OH} of Et-CH, estimated from the O2···O1′ distance, is ca. 3550–3500 cm^{-1}, while the observed value was ca. 3420 and 3330 cm^{-1}. The decrease in the wavenumber of ν_{OH} is an indication of the bifurcated H-bond [14].

In solid Et-CH, the period along the 2_1 axis is 594 pm, and in each of the six crystals of chloral hemiacetals mentioned above it falls in a narrow region of 580–610 pm. The period along the 2_1 axis is thus an indication of the presence of the H-bonded chain structure. Then, the crystal data of nHp-CH (monoclinic, space group $P2_1$, and b = 584.0 pm) indicate that the crystal of this compound contains the H-bonded chain structure common to the chloral hemiacetals mentioned above.

T_1 of ^{35}Cl NQR in Me- and Et-CH

The sharp decrease in T_1 with increasing temperature observed above 240–250 K is attributable to the onset of reorientation of the CCl_3 group and is at higher temperatures approximately described by [15]:

$$T_1^{-1} = b \exp(-V_0/RT), \tag{1}$$

where V_0 is the potential barrier hindering the reorientation. The values of V_0 calculated from the slope of the T_1 vs. $1/T$ curves are given in Table 3. The magnitudes of V_0 obtained for Me- and Et-CH are comparable to those reported for the other chloral hemiacetals [3, 4].

In the lower temperature region T_1^{-1} obeys approximately the T^2 law

$$1/T_1 = kT^2. \tag{2}$$

Then, the spin lattice relaxation is considered to be governed by lattice vibrations [15].

T_1 of ^{35}Cl NQR in nHp-CH

The temperature dependence of T_1 above ca. 270 K can be described by (1) with $V_0 = 32 \pm 3$ kJ/mol. The value of V_0 is comparable to those found for CCl_3 groups in Me- and Et-CH and other chloral hemiacetals [3, 4].

In the range from ca. 160 to 270 K, the behavior of T_1 is anomalous. A similar phenomenon has been found for cycHx-CH in almost the same range [3]. According to the method applied to the analysis of the T_1 behavior in cycHx-CH, the parts of the spin lattice relaxation rate ($1/T_1$) of nHp-CH calculated by (2) were subtracted from the observed values of $1/T_1$. The results shown in Fig. 5 suggest the presence of T_1 minima superimposed on the sharp decrease of T_1 due to the reorientation of the CCl_3 group. Then, the T_1 vs. $1/T$ curves with T_1 minima shown in Fig. 6 were extracted as differences between the T_1 shown in Fig. 5 and those calculated by using (1). The curves in Fig. 6 can be approximately described by the equation [15]

$$\frac{1}{T_1} = \frac{C\tau}{1 + (\omega\tau)^2}, \tag{3}$$

where $\tau = \tau_0 \exp(E_m/RT)$ and C is a constant. This expression is based on the assumption that for some atom (or group) there are two equivalent sites (potential wells) separated by a barrier and the atom (or the

Table 3. The values of V_0 for Me-, Et-, and nHp-CH.

	Me-CH	Et-CH	nHp-CH
V_0 (kJ mol^{-1})	39 ± 3	37 ± 1	32 ± 3

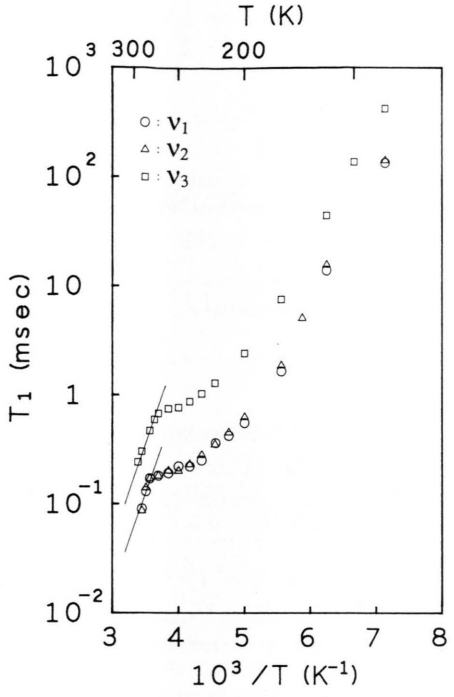

Fig. 5. Temperature dependence of T_1 obtained by subtracting T_1^{-1} calculated by (2) from the observed values.

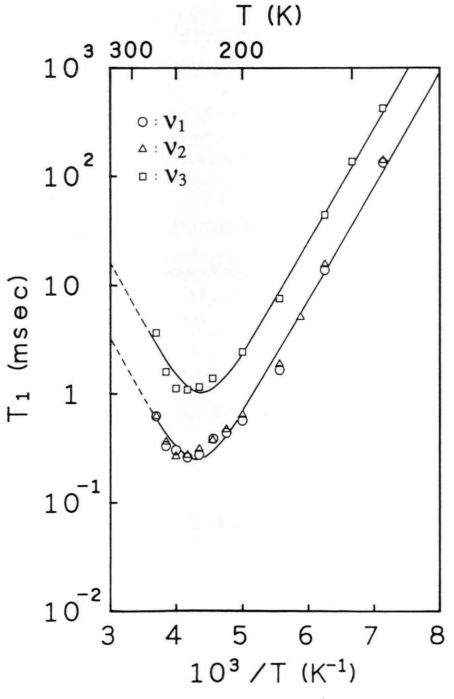

Fig. 6. Temperature dependence of T_1 obtained by subtracting T_1^{-1} calculated by (1) and (2) from the observed values. The solid and broken curves are calculated by (3).

group) jumps between them with a frequency comparable to the NQR frequency, producing a fluctuation of the EFG. When the potential wells are not equivalent (asymmetric) and the depths of the two sites 1 and 2 are E_1 and E_2, respectively, one should use the following equation instead of (3) [16, 17]:

$$\frac{1}{T_1} = \frac{4a}{(1+a)^2} \cdot \frac{C\tau}{1+(\omega\tau)^2}, \tag{4}$$

where $a = \exp\left((E_1 - E_2)/RT\right)$.

In the present work we applied (3) because (i) in the case of cycHx-CH, where the potential well is presumably asymmetric, the analysis using (3) gave almost the same results as those obtained by (4) and (ii) the exact crystal structure of nHp-CH was unknown. The following values were obtained for E_m and τ_0: $E_m \approx 20$ kJ/mol, $\tau_0 = 1.34 \times 10^{-13}$ s for ν_1 and ν_2, and 1.13×10^{-13} s for ν_3. The solid lines in Fig. 6 denote the values of T_1 calculated by (3) with τ_0 and E_m as obtained above.

A dynamic disorder of hydrogen atoms due to their jumping motions in the hydrogen bonded chains has been proposed as a probable source of the fluctuation of EFG responsible for the T_1 minima of the ^{35}Cl NQR found for nB-CH and cycHx-CH [2, 3].

Although the exact crystal structure of nHp-CH is not available, the H-bonded chain structure in the crystal is considered to be similar to those in nB- and cycHx-CH. The splitting of the ν_{OH} IR band of nHp-CH indicates that there may be two sites between which the hydrogen atom jumps. Then, one could assume the same mechanism to interpret the unusual T_1 minimum found for nHp-CH. The fact that the T_1 minima of ν_1 and ν_2 are equal and are smaller than

Table 4. The observed temperature coefficients of ^{35}Cl NQR frequencies ($C_T = (d\nu/dT)/\nu_q$ *) of Me-, Et-, and nHp-CH and the contribution due to the reorientation of the CCl_3 group (C_T(calc.)).

	$C_T/10^{-3}$ K^{-1}		
	Me-CH	Et-Ch	nHp-CH
ν_1	0.22	0.12	0.14
ν_2	0.17	0.13	0.12
ν_3	0.13	0.17	0.10
	C_T (calc.) **		
	0.071	0.075	0.087

* ν_q denotes the NQR frequency of the static lattice.
** The temperature coefficients calculated from the observed values of V_0 (see text).

that of ν_3 may reflect the local arrangement of the hydrogen (in OH) and the three chlorine atoms.

It should be mentioned that T_1 of ν_3 seems to be longer than T_1 of ν_1 and ν_2 even at higher temperatures. The reason of this observation can not be specified because compound melts at 305 K.

From the H-bonded chain structure found in the Et-CH crystal one may expect a similar jumping motion of hydrogen atoms in this compound. For Et-CH, as well as for pCB-CH [4], however, the unusual T_1 minimum was not observed in the temperature range investigated. This might indicate that the fluctuations of the EFG are too small to produce an appreciable drop of T_1, or that the frequency spectrum of the jumping motion is far away from the NQR frequency in the temperature range investigated.

Temperature Dependence of the ^{35}Cl NQR Frequency

Table 4 lists the temperature coefficients (C_T) of the NQR frequencies calculated from our previous data [6]. The contribution of the reorientation of CCl_3 to C_T was calculated by the equation [18]

$$C_T = (d\nu/dT)/\nu_q = -R/3V_0, \quad (5)$$

where ν_q is the NQR frequency of the static lattice. The values of C_T obtained from V_0 by using (5) are also listed in Table 4. It is clear that the reorientation of the CCl_3 group explains only part of C_T and hence other modes of molecular motions are also responsible for C_T.

Acknowledgement

This work was supported in part by a Grant-in Aid for Scientific Research from Ministry of Education, Science and Culture. We are grateful to Miss A. Shono and Mr. T. Isono for their help in the X-ray works.

[1] H. Chihara and N. Nakamura, Adv. Nucl. Quad. Reson. **4,** 1 (1980).
[2] M. Hashimoto, T. Isono, H. Niki, and T. Higa, Z. Naturforsch. **45a,** 472 (1990).
[3] H. Niki, H. Kyan, T. Hamagawa, R. Igei, T. Isono, and M. Hashimoto, Z. Naturforsch. **47a,** 299 (1992).
[4] M. Hashimoto, T. Isono, N. Yomesaka, H. Niki, H. Kyan, and T. Hamagawa, Z. Naturforsch. **47a,** 293 (1992).
[5] Beilstein, Band I, S. 619.
[6] M. Hashimoto and Al. Weiss, Ber. Bunsenges. Phys. Chem. **86,** 134 (1982).
[7] P. Main, S. E. Hull, L. Lessinger, G. Germain, J. P. Declercq, and M. M. Woolfson MULTAN 78, A System of Computer Programs for the Automatic Solution of Crystal Structures from X-ray Diffraction Data. Univ. of York, England, and Louvain, Belgium 1978.
[8] T. Ashida, The Universal Crystallographic Computing Systems – Osaka, HBLS-V, p. 53. The Computer Center, Osaka Univ., Japan 1979.
[9] International Tables for X-ray Crystallography, Kynoch Press, Birmingham 1974, Vol. 4.
[10] T. Sakurai and K. Kobayashi, Rikagaku Kenkyusho Hokoku **55,** 69 (1979).
[11] Y. Mido and M. Hashimoto, J. Mol. Struct. **129,** 253 (1985).
[12] MOPAC Ver. 6, J. J. P. Stewert, QCPE Bull. **9,** 10 (1989); Revised by H. Chawanya for VAX machine.
[13] M. Hashimoto, T. Isono, and K. Mano, to be published.
[14] K. Nakamoto, M. Margoshes, and R. E. Rundle, J. Amer. Chem. Soc. **77,** 6480 (1950).
[15] D. E. Woessner and H. S. Gutowsky, J. Chem. Phys. **39,** 440 (1963).
[16] N. E. Ainbinder, G. A. Volgina, I. A. Kjuntsel, V. A. Mokeeva, A. N. Osipenco, and G. B. Soifer, Sov. Phys. JETP **50,** 348 (1979).
[17] N. E. Ainbinder, I. A. Kjutsel, V. A. Mokeeva, A. N. Osipenco, G. B. Soifer, and I. G. Shaposhnikov, J. Mol. Struct. **58,** 349 (1980).
[18] M. Hashimoto, Anal. Instrum. **13,** 160 (1975).